Heat capacity measurements of two-dimensional self-assembled hexadecanethiol monolayers on polycrystalline gold

Z. S. Zhang, O. M. Wilson, M. Yu. Efremov, E. A. Olson, and P. V. Braun
Materials Science Department, University of Illinois, Urbana, Illinois 61801

W. Senaratne and C. K. Ober
Materials Science and Engineering, Cornell University, Ithaca, New York 14850

M. Zhang and L. H. Allen[a)]
Materials Science Department and CSL, University of Illinois, Urbana, Illinois 61801

(Received 5 March 2004; accepted 28 April 2004; published online 10 June 2004)

The melting characteristics of hexadecanethiol two-dimensional self-assembled monolayers (SAMs) grown on polycrystalline Au surfaces are obtained via heat capacity measurements using nanocalorimetry at scanning rates of ~30 000 °C/s. The analyzed amount of alkanethiol in the form of SAMs is typically in the 10^{-11} mol range. Melting occurs over a broad (full width on the half height ~100 °C) temperature range with a melting temperature of about 70 °C, if the alkanethiol is partially desorbed from the Au surface during thermal treatment. SAMs in their as-deposited state without desorption have melting temperatures above 100 °C. The heat of fusion is about 20 kJ/mol. Partial desorption of the alkanethiol is directly observed. The melting characteristics of three-dimensional SAMs on Au nanoparticles are comparable to earlier studies using conventional calorimetry. © *2004 American Institute of Physics*. [DOI: 10.1063/1.1764938]

In recent years, self-assembled monolayers (SAMs) have generated great interest[1] both in the fundamental issues of two-dimensional (2D) melting[2] and in applications for molecular electronics,[3] diffusion barriers in microelectronic device fabrication,[4] corrosion control,[5] and lubrication.[6] The *n*-alkanethiolate SAMs on Au surface serve as the model SAMs system. The thermodynamic and structure characteristics of SAMs, in particular the order–disorder (melting) phase transitions, are essential for developing technological applications. This transition has been studied using a variety of experimental techniques.[7–11]

Calorimetry is the standard method for phase transition studies.[12] It provides unique characteristics of the transition such as enthalpy and entropy as well as the specific heat of the phases. Although conventional differential scanning calorimetry (DSC) is routinely used for thin film characterization,[13] it is not sensitive enough for characterizing SAMs grown on a planar surface (2D SAMs), where the amount of alkanethiol is only in the 10^{-11} mol range.[12] Previously, conventional DSC was used to observe melting of SAMs on alkanethiol-coated Au nanoparticles (3D SAMs) in the form of dry powder.[14,15] However, applying the results of 3D SAMs to predict the characteristics of 2D SAMs is difficult due to the effects of intercalation between adjacent clusters which may occur in powder samples.[12,15]

Advances in micro-electromechanical systems (MEMS) thin-film differential scanning calorimetry (TDSC)[16,17] or nanocalorimetry allow us to directly measure the heat capacity $C_p(T)$ of 2D SAMs. Recently this method was used to study other ultra thin film polymer and metal samples[18,20] Calorimetry investigations of 2D SAMs have the advantage over 3D SAMs because they avoid the complications of cluster–cluster interdigitation and size-dependent melting effects due to the dispersion of the nanoparticles size. Effects of interdigitation are not expected for 2D SAMs.

In this letter, we report $C_p(T)$ measurements of 2D SAMs on planar polycrystalline Au samples. We also measure 3D SAMs synthesized from solution in order to compare with previous studies using conventional DSC.[14,15] We obtain the peak melting temperature T_p, heat of fusion H_m, and desorption information from the $C_p(T)$ data. Hexadecanethiol ($CH_3(CH_2)_{15}SH$) SAMs (abbreviated as C_{16} SAMs) were chosen in this study because the long chain alkanethiols ($>C_{14}$) easily form well-ordered monolayers.[8,9]

The nanocalorimetry method is reported in detail elsewhere.[17,18,21] The MEMS-based sensor is microfabricated on a Si wafer as shown in the inset of Fig. 1. In this work, Al is selected for the metallization layer, because alkanethiolate SAMs are not expected to grow on the native Al oxide layer,[22] which forms spontaneously on exposure to air.[23] Sensors made with Pt metallization show similar but less reproducible results. Transmission electron microscopy (TEM)

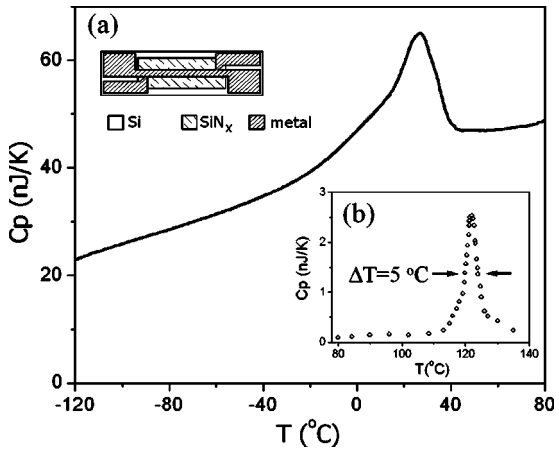

FIG. 1. $C_p(T)$ curve for 3D SAMs on Au nanoparticles using the nanocalorimeter technique at a scan rate of 33 000 °C/s. Inset (a): top-view schematic diagram of the MEMS-based sensor. Inset (b): $C_p(T)$ curve for a single crystal polyethylene measured by the same type calorimeter (Ref. 20), which demonstrates the sensitivity and temperature resolution of the TDSC.

[a)]Electronic mail: l-allen9@uiuc.edu

JEOL 2010F is used to image the Au nanoparticles (3D SAMs) and ellipsometry (Focus Ellipsometer FE-III, Rudolph Technologies, Inc.) is used to measure the average thickness of the 2D SAMs.

Sample preparation for 2D SAMs proceeds as follows: first, a 4 nm Cr (adhesion layer) and a 75 nm Au layer are sequentially thermally deposited onto the SiN_x side of the sensors using a shadow mask. Then the baseline TDSC and ellipsometry measurements are obtained. Finally, the sample sensor is immersed into a 1 mM hexadecanethiol in ethanol solution for 48 h at room temperature, after which it is extracted from the solution and thoroughly rinsed with ethanol.[24] The colloid dispersion of 3D SAMs on alkanethiol-coated Au nanoparticles is synthesized following the standard method[25] and then deposited directly onto the sensor using a pipette. Commercial hexadecanethiol (Aldrich, >95% purity) is used without further purification.

All TDSC measurements are performed in a vacuum chamber (1×10^{-8} Torr). Both the sample and reference sensors are mounted on a copper stage, which is cooled by liquid nitrogen (LN2). TDSC measurements are obtained using ultrafast scanning rates (heating: $\sim30\,000\,^{\circ}C/s$ and cooling: $\sim5\,000\,^{\circ}C/s$) from LN2 temperature. Multiple scans were taken at 2 s intervals.

The amount of alkanethiol in the 2D SAMs was determined using three different methods: (1) C_p measurements, (2) ellipsometry, and (3) the surface coverage on the Au surface area. Using C_p measurements of the liquid and solid states of the SAMs, we estimate the amounts of alkanethiol assuming bulk values of specific heat of hexadecane.[26] In addition, the alkanethiol amount is also estimated using thickness values from ellipsometry and the density of bulk hexadecanethiol.[27] We also estimate the amount of alkanethiol by assuming that the 2D SAM completely covers (100%) the measured sample area with a uniform molecular area density of the alkanethiol (0.214 nm^2/molecule).[28] The average amount of the alkanethiol estimated by all these methods is $1.42\pm0.16\times10^{-11}$ mol.

Figure 1 shows a calorimetric curve of 3D SAMs. (7×10^{-11} mol of alkanethiol). Typical 3D SAMs exhibit a somewhat broad [full-width-on-the-half-height (FWHH) $\sim35\,^{\circ}C$] endothermic peak with peak temperature $T_{p3D}\sim25\pm3\,^{\circ}C$ and a heat of fusion $H_{m3D}\sim16\pm5$ kJ/mol. The calorimetric scans up to 100 °C are reproducible over 100 scans and the effects of desorption are not apparent. These results are consistent with previous works ($T_p\sim30\,^{\circ}C, H_{m3D}=14$ kJ/mol)[15] and ($T_p=41\,^{\circ}C, H_{m3D}=13.8\pm0.8$ kJ/mol)[29] for 3D SAMs dry powder samples ($\sim2\times10^{-5}$ mol of alkanethiol) using conventional DSC[14,15] at $\sim0.1\,^{\circ}C/s$ scan rate. Our sample is $\sim10^6$ smaller than used for conventional DSC work.

The broadness of the transition peak cannot be explained by the instrumentation broadening for the extremely small sample. The inset to Fig. 1, demonstrates the resolution of the TDSC technique for small samples, a C_p measurement of a single crystal polyethylene sample[20] which has ~100 times smaller amount of material than the samples used for our 2D SAMs measurements. The narrow (FWHH $\sim5\,^{\circ}C$) melting peak[20] ensures that the instrumentation broadening is negligible. The broadness of the peak may be partially due to the variation in particle size coupled with the size-dependent melting temperature of 3D SAMs.[30]

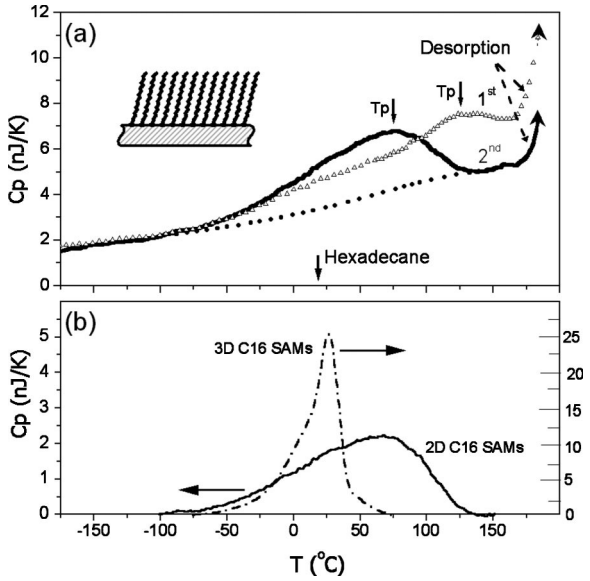

FIG. 2. (a) $C_p(T)$ data of the first ($Tp>100\,^{\circ}C$) and second ($T_p\sim70\,^{\circ}C$) scans with a maximum scanning temperature to 200 °C for 2D SAMs on planar Au surface. The large shift (50 °C) of the melting temperature from the first scan to the second scan is due to desorption of the alkanethiol (see sharp onset of C_p at 170 °C). The heat of fusion for the partially desorbed sample (second scan) is $H_{m2D}\sim20$ kJ/mol. Inset: the schematic of 2D SAMs on planar Au surface. (The square dots represent the expected baseline for the specific heat of SAMs.) (b) Comparison of the C_p data for both 2D and 3D SAMs after the baseline has been subtracted.

One complication in analyzing calorimetry measurements of 3D SAMs is the effect of interdigitation between neighboring clusters during calorimetry. Interdigitation makes it difficult to separate the melting properties due to cluster–cluster overlap from the intrinsic melting properties of the SAMs on individual separated nanoparticles. Previous work[15] suggests that most of the transition enthalpy in 3D SAMs is due to the interdigitation. Investigation of 2D SAMs, made possible by TDSC technique, allows one to decouple SAMs melting from the interdigitation effect.

Typical $C_p(T)$ curves for 2D SAMs are shown in Fig. 2 of the first and second scans to 200 °C. The broad endothermic peak with FWHH ~100 °C of the calorimetric curves starting at ~100 °C and persisting up to about 150 °C corresponds to the endothermic peak on the 3D SAM $C_p(T)$ data (Fig. 1). The sharp endothermic signal at the end of the scans starting at ~170 °C is attributed to the desorption process of alkanethiol. While T_p for the first scan is about 120 °C, the T_p for the second scan is substantially lower by about 50 °C. The transition temperature for 2D SAMs is consistent with the value of 80 °C, found for full coverage 2D SAMs.[8]

Desorption during the first scan is considered to be the reason for the large shift of the melting peak to a lower temperature in the second scans. We estimate that 5% of the alkanethiol desorbs due to the first scan. This estimate is made using the change in C_p for the solid film between the first and second scans. The large effect of desorption on the melting characteristics of SAMs also has been observed previously in C10 2D SAMs.[31,32] It has been shown for C_{10} 2D SAMs, that the highest value of T_p occurs at coverage close to 100%. Furthermore, a few percent decrease in the coverage causes a substantial drop in T_p (e.g. $\Delta T_p=50\,^{\circ}C$ decrease in T_p occurs by changing the coverage from 100 to 95%). If coverage decreases even further, T_p stabilizes. In our case the

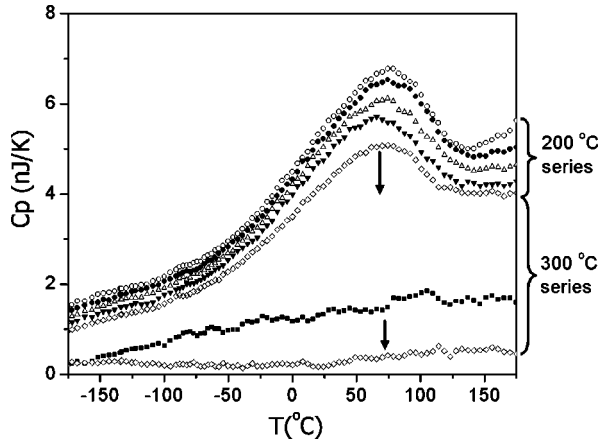

FIG. 3. A series of $C_p(T)$ curves of multiple scans with two different maximum scanning temperatures. The 200 °C series (LN2 temperature to 200°C) shows the gradual desorption of 2D SAMs which is indicated by the decrease in $C_p(T)$ data. There is a 30% loss of mass and a 40% decrease in the heat (area under the curve) of melting during this series. After the 200 °C series the sample is scanned to 330 °C (LN2 temperature to 330 °C). Most of the remaining alkanethiol molecules desorb in the first few pulses during these high temperature scans.

difference between T_p of the first and second scans is also about 50 °C. This parallelism to C_{10} SAMs results also implies that the coverage probed by the first scan is close to 100%. The desorption process also occurs during the second and subsequent scans (see Fig. 3), but to a lesser degree and does not cause a noticeable peak shift, which is also consistent with the work on C_{10} 2D SAMs, if we suppose the same plateau on the T_p versus coverage dependence. The large difference between 2D and 3D SAMs has also been shown by simulations[30] in the C12 system: $T_{p3D}=21$ °C(FWHH ~ 35 °C) and $T_{p2D}=130$ °C(FWHH ~ 100 °C).

The measured value of heat of fusion $H_{m2D}(20\pm4$ kJ/mol) is nearly equal to $H_{m3D}(16\pm5$ kJ/mol). However, both H_{m2D} and H_{m3D} are considerably lower than the bulk value for pure hexadecane (53 kJ/mol).[26] This observation is also supported by molecular dynamics simulations[30] where H_{m3D} for C_{12} SAMs on Au_{140} and Au_{1289} clusters are found to be ~ 20 kJ/mol, which is significantly smaller than the bulk value for dodecane, $H_{m\text{-bulk}}(40$ kJ/mol).[26] One explanation for why $H_{m2D} < H_{m\text{-bulk}}$ is that only part of the film (e.g., a portion of the chain) is involved in the melting process.[15,33] Using the estimation that the heat of fusion is 3–4 kJ per mole of CH_2 groups,[15,33] the effective number of CH_2 segments involved in the melting is only four to six per chain. On the microscopic level H_{m2D} will be associated with the population and energetics of the generation of gauche defects over the broad temperature range (formation energy of a gauche defect is about 2 kJ/mol-defect for a free alkane).[34] Another explanation[29] is that melting process of SAMs should also be compared to the gel-to-liquid crystalline transition.

In summary, TDSC shows that the temperature of the transition for 2D SAMs is much higher and broader than 3D SAMs and the heat of fusion for 2D and 3D SAMs are comparable but much lower than for bulk alkanethiol. Melting characteristics of the 3D SAMs are comparable with earlier studies using conventional DSC.

The authors acknowledge P. Infante of the Cornell Nanofabrication Facility. This research is supported by NSF 0108694 and ACS-PRF No. 37027-AC7. Support for O.M.W. and P.V.B. the microanalysis tasks were under DEFG02-91ER45439.

[1] A. Bishop and R. Nuzzo, Curr. Opin. Colloid Interface Sci. **1**, 127 (1996); R. Nuzzo and D. Allara, J. Am. Chem. Soc. **105** , 4481 (1983).
[2] M. J. Hostetler, W. L. Manner, R. G. Nuzzo, and G. S. Girolami, J. Phys. Chem. **99**, 15269 (1995).
[3] W. Wang, T. Lee, and M. A. Reed, Phys. Rev. B **68**, 035416 (2003).
[4] P. G. Ganesan, J. Gamba, A. Ellis, R. S. Kane, and G. Ramanath, Appl. Phys. Lett. **83**, 3302 (2003); J. A. Mayer and S. S. Lau, *Electronic Materials Science: For Integrated Circuits in* Si *and* GaAs (Macmillan, New York, 1990).
[5] G. M. Whitesides and P. E. Laibinis, Langmuir **6**, 87 (1990).
[6] C. E. D. Chidsey and D. N. Loiacono, Langmuir **6**, 682 (1990).
[7] A. Badia, R. Back, and R. B. Lennox, Angew. Chem., Int. Ed. Engl. **33**, 2332 (1994).
[8] P. Fenter, P. Eisenberger, and K. Liang, Phys. Rev. Lett. **70**, 2447 (1993).
[9] F. Bensebaa, T. Ellis, A. Badia, and R. Lennox, Langmuir **14**, 2361 (1998).
[10] L. H. Dubois, B. R. Zegarski, and R. G. Nuzzo, J. Electron Spectrosc. Relat. Phenom. **54/55**, 1143 (1990); R. G. Nuzzo, E. M. Korenic, and L. H. Dubois, J. Chem. Phys. **93**, 767 (1990).
[11] Y. Qian, G. Yang, J. Yu, T. A. Jung, and G. -Y. Liu, Langmuir **19**, 6056 (2003); G. E. Poirier, W. P. Fitts, and J. M. White, *ibid.* **17**, 1176 (2001); E. Delamarche, B. Michel, H. Kang, and C. Gerber, *ibid.* **10**, 4103 (1994).
[12] A. Badia, R. B. Lennox, and L. Reven, Acc. Chem. Res. **33**, 475 (2000).
[13] J. M. E. Harper, L. A. Clevenger, E. G. Colgan, C. Cabral, Jr., and B. Arcot, Interface Control of Electrical, Chemical and Mechanical Properties Symposium, 1994, p. 307.
[14] A. Badia, S. Singh, L. Demers, L. Cuccia, G. R. Brown, and R. B. Lennox, Chem.-Eur. J. **2**, 359 (1996).
[15] R. H. Terrill, T. A. Postlethwaite, C. -H. Chen, C. -D. Poon, A. Terzis, A. Chen, J. E. Hutchison, M. P. Clark, G. Wignall, J. D. Londono, R. Superfine, M. Falvo, C. S. Johnson, Jr., E. T. Samulski, and R. W. Murray, J. Am. Chem. Soc. **117**, 12537 (1995).
[16] M. Yu. Efremov, E. A. Olson, M. Zhang, F. Schiettekatte, Z. S. Zhang, and L. H. Allen, Rev. Sci. Instrum. **75**, 179 (2004).
[17] E. A. Olson, M. Yu. Efremov, M. Zhang, Z. S. Zhang, and L. H. Allen, J. Microelectromech. Syst. **12**, 355 (2003).
[18] M. Yu. Efremov, E. A. Olson, M. Zhang, and L. H. Allen, Thermochim. Acta **403**, 37 (2003).
[19] M. Yu. Efremov, E. A. Olson, M. Zhang, Z. S. Zhang, and L. H. Allen, Phys. Rev. Lett. **91**, 085703 (2003); S. L. Lai, J. Y. Guo, V. Petrova, G. Ramanath, and L. H. Allen, *ibid.* **77**, 99 (1996); M. Yu. Efremov, F. Schiettekatte, M. Zhang, E. A. Olson, A. T. Kwan, R. S. Berry, and L. H. Allen, *ibid.* **85**, 3560 (2000); M. Zhang, M. Yu. Efremov, F. Schiettekatte, E. A. Olson, A. T. Kwan, S. L. Lai, T. Wisleder, J. E. Greene, and L. H. Allen, Phys. Rev. B **62**, 10548 (2000).
[20] A. T. Kwan, M. Yu. Efremov, E. A. Olson, F. Schiettekatte, M. Zhang, P. H. Geil, and L. H. Allen, J. Polym. Sci., Part B: Polym. Phys. **39**(11), 1237 (2001).
[21] M. Yu. Efremov, E. A. Olson, M. Zhang, S. Lai, F. Schiettekatte, Z. S. Zhang, and L. H. Allen, Thermochim. Acta **412**, 13 (2004).
[22] P. E. Laibinis, J. J. Hickman, M. S. Wrighton, and G. M. Whitesides, Science **245**, 845 (1989).
[23] M. T. A. Saif, S. Zhang, A. Haque, and K. J. Hsia, Acta Mater. **50**, 2779 (2002).
[24] C. D. Bain, E. B. Troughton, Y. Tao, J. Evall, G. M. Whitesides, and R. G. Nuzzo, J. Am. Chem. Soc. **111**, 321 (1989).
[25] M. Brust, M. Walker, D. Bethell, D. J. Schiffrin, and R. Whyman, J. Chem. Soc., Chem. Commun. **7**, 801 (1994).
[26] ATHAS Data Bank (1992).
[27] C. L. Yaws, *Chemical Properties Handbook* (McGraw-Hill, New York, 1999).
[28] A. Ulman, Chem. Rev. (Washington, D.C.) **96**, 1533 (1996).
[29] A. Badia, L. Cuccia, L. Demers, F. Morin, and R. B. Lennox, J. Am. Chem. Soc. **119**, 2682 (1997).
[30] W. D. Luedtke and U. Landman, J. Phys. Chem. B **102**, 6566 (1998).
[31] F. Schreiber, Prog. Surf. Sci. **65**, 151 (2000).
[32] R. Nuzzo, L. Dubois, and D. Allara, J. Am. Chem. Soc. **112**, 558 (1990).
[33] J. Watanabe, H.Ono, I.Uematsu, and A.Abe,Macromolecules **18**, 2141 (1985).
[34] N. F. Nagle and H. L. Scott, Phys. Today **31**, 38 (1978).